

Conditions for superconductivity in the electron-doped copper-oxide system, $(\text{Nd}_{1-x}\text{Ce}_x)_2\text{CuO}_{4+\delta}$

Y. Tanaka^a, T. Motohashi^a, M. Karppinen^{a,b,*}, H. Yamauchi^a

^aMaterials and Structures Laboratory, Tokyo Institute of Technology, Yokohama 226-8503, Japan

^bLaboratory of Inorganic and Analytical Chemistry, Helsinki University of Technology, FI-02015 TKK, Finland

Received 6 June 2007; received in revised form 16 October 2007; accepted 27 November 2007

Available online 5 December 2007

Abstract

We report systematic studies on the relations among the Ce^{IV} -for- Nd^{III} substitution level (x), oxygen-partial pressure (P_{O_2}), oxygen content ($4 + \delta$), lattice parameters (a , c) and superconductivity characteristics (T_c , volume fraction) in the $(\text{Nd}_{1-x}\text{Ce}_x)_2\text{Cu}_{1-y}\text{O}_{4+\delta}$ system which includes electron-doped superconductors. Independent of the Ce-doping level x , samples synthesized in air are found oxygen deficient, i.e. $\delta < 0$. Nevertheless, reductive annealing is needed to induce superconductivity in the air-synthesized samples. At the same time, the amount of oxygen removed upon the annealing is found very small (e.g. 0.004 oxygen atoms per formula unit at $x = 0.075$), and consequently the effect of the annealing on the valence of copper (and thereby also on the electron doping level) is insignificant. Rather, the main function of the reductive annealing is likely to repair the Cu vacancies believed to exist in tiny concentrations (y) in the air-synthesized samples.

© 2007 Elsevier Inc. All rights reserved.

Keywords: High- T_c superconductor; $(\text{Nd}, \text{Ce})_2\text{CuO}_4$; Electron doping; Reductive annealing; Oxygen content; Iodometric titration

1. Introduction

Since discovered in 1989 [1], electron-doped high- T_c copper-oxide superconductors, $(R,\text{Ce})_2\text{CuO}_4$ with $R = \text{Pr}$, Nd or Sm , have been in the focus of continuous research efforts. Nevertheless there still remain many questions to be answered related particularly to their peculiar doping characteristics, that is, the definite requirements in terms of x , y and δ for the appearance of superconductivity in $(R_{1-x}\text{Ce}_x)_2\text{Cu}_{1-y}\text{O}_{4+\delta}$. The $(R,\text{Ce})_2\text{CuO}_4$ phases crystallize in a so-called T' structure [2] with an alternating stacking of fluorite-structured $(R,\text{Ce})_2\text{O}_2$ layers and apical-oxygen-free CuO_2 planes. Successful induction of superconductivity seems to require that a proper concentration of electrons is generated through partial substitution of trivalent R by tetravalent Ce and—simultaneously—the as-air-synthesized samples should be reduced through a

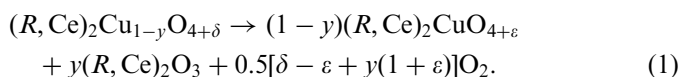
low-oxygen-partial-pressure annealing [3]. The double requirement is in clear contrast to the hole-doped copper-oxide counterpart, the $(\text{La}_{1-x}\text{Sr}_x)_2\text{CuO}_{4+\delta}$ system (of the T structure [4]), which shows superconductivity simply upon an introduction of a sufficient concentration of holes, as achieved either through oxygen doping or by means of divalent-for-trivalent cation substitution. Moreover, the Ce-content range of $x \approx 0.07$ – 0.09 within which superconductivity appears (after an appropriate post-synthesis annealing) in $(R_{1-x}\text{Ce}_x)_2\text{Cu}_{1-y}\text{O}_{4+\delta}$ [3,5,6] is much narrower than that of Sr ($x \approx 0.03$ – 0.125) in the hole-doped $(\text{La}_{1-x}\text{Sr}_x)_2\text{CuO}_{4+\delta}$ superconductor system [7].

Most of the previous studies agree that the post-synthesis low-oxygen-partial-pressure annealing plays an important role in the course of superconductorizing electron-doped $(R,\text{Ce})_2\text{CuO}_4$ oxides. However, the reason for the necessity of this has remained controversial. It has been suggested that (i) complete removal of the minute amounts of oxygen atoms from the otherwise vacant apical site is crucially important in order to decrease magnetic correlation [8], impurity scattering [9] and/or disorder effect [10], and alternatively that (ii) creation of oxygen vacancies [11,12]

*Corresponding author. Laboratory of Inorganic and Analytical Chemistry, Helsinki University of Technology, FI-02015 TKK, Finland. Fax: +358 9 462 373.

E-mail address: Maarit.Karppinen@tkk.fi (M. Karppinen).

or (iii) filling the Cu vacancies in the CuO_2 plane [13] is crucially important in order to suppress the long-range antiferromagnetic interactions and/or disorder within the plane. Accordingly, some neutron diffraction studies have ended up with a conclusion that the oxygen atoms that are removed upon the reductive annealing are those located at the defect apical oxygen site [14–16], whereas others have concluded that the reduction creates oxygen vacancies in the CuO_2 plane [17–20]. Oxygen vacancies may also appear in the fluorite-structured $(R,\text{Ce})_2\text{O}_2$ layer [14,15,17,20], especially in samples with low Ce contents ($x < 0.05$) [11,12]. Moreover, most recent works have revealed that the as-synthesized samples tend to be slightly Cu deficient; then upon the reductive annealing the Cu-deficient $(R,\text{Ce})_2\text{Cu}_{1-y}\text{O}_{4+\delta}$ phase separates into essentially cation-stoichiometric $(R,\text{Ce})_2\text{CuO}_{4+\varepsilon}$ superconductive phase and a Cu-free minority phase of $(R,\text{Ce})_2\text{O}_3$ of the cubic fluorite structure, i.e. [13]:



Changes in the overall oxygen content upon the post-synthesis low-oxygen-partial-pressure annealing have been followed by means of thermogravimetric (TG) [13,21–27] and iodometric titration [28–33] analyses. These studies have concluded that the amount of oxygen lost upon the reductive annealing is relatively small. Also agreed is that the magnitude of oxygen loss decreases with Ce content [18,21,25,26,28,29,32]. However, exact estimates for the amount of lost oxygen vary from 0.01 to 0.04 oxygen atoms *per* formula unit for samples with a sufficient Ce-doping level ($x = 0.05\text{--}0.08$) [13,18,21,25–29,31,32]. Absolute oxygen content values reported for oxygen-reduced superconductive samples are controversial too: some groups have concluded values lower than 4.00 [28,31], whereas others suggest values higher than 4.00 [29,30,32].

Here we readdress the yet puzzling questions related to the oxygen nonstoichiometry and electron doping in the $(R,\text{Ce})_2\text{CuO}_{4+\delta}$ system. For this purpose, an extensive series of high-quality $(\text{Nd}_{1-x}\text{Ce}_x)_2\text{Cu}_{1-y}\text{O}_{4+\delta}$ samples with precisely controlled and accurately analyzed oxygen contents was systematically investigated.

2. Experimental

A series of polycrystalline samples of $(\text{Nd}_{1-x}\text{Ce}_x)_2\text{Cu}_{1-y}\text{O}_{4+\delta}$ with x ranging from 0.00 to 0.10 was prepared employing a wet-chemical method in which the solution-mixed metal ions are uniformly precipitated using ethylenediaminetetraacetic acid (EDTA) as a chelating agent [34]. Compared with the conventional solid-state reaction method the EDTA method yields more homogeneous samples at lower synthesis temperatures. Accordingly the grain size of the product is smaller and more uniform. Stoichiometric (i.e. $y = 0$) amounts of the starting powders, Nd_2O_3 (heated to 850°C *prior* to use to get rid of absorbed

water/carbon dioxide), $\text{Ce}(\text{NO}_3)_3 \cdot 6\text{H}_2\text{O}$ and CuO , were dissolved in aqueous 2 M HNO_3 solution from which the metal ions were chelated with aqueous EDTA/ NH_3 solution containing a 50% molar excess of EDTA against the total amount of metal ions. The pH value was then adjusted to 8–9 (with HNO_3 and/or NH_3 solutions) to obtain a clear blue solution. After stirring at $\sim 80^\circ\text{C}$ for approximately 30 min to promote the chelation, the solution was evaporated and the gel was burned. The resultant raw ash was pressed into pellets and fired at 1050°C for 12 h in air, followed by furnace cooling to room temperature at a rate of $5^\circ\text{C}/\text{min}$.

For oxygen reduction, the as-air-synthesized samples were annealed at 1000°C for 24 h under oxygen partial pressures (P_{O_2}) ranging from 10^{-5} to 10^{-2} atm. During the annealing the P_{O_2} value was precisely controlled using a gas mixer and an oxygen densitometer equipped with a ZrO_2 sensor. After the annealing the sample was furnace-cooled down to room temperature in the same atmosphere with the rate of $10^\circ\text{C}/\text{min}$.

All the samples were examined with X-ray powder diffraction (XRD; Rigaku: RINT2000 equipped with a rotating anode; $\text{CuK}\alpha$ radiation) to investigate the phase composition and to determine the lattice parameters. Refinement of the lattice parameters was performed in tetragonal space group, $I4/mmm$, using the software JANA2000 [35]. Superconductivity properties were measured for powdered samples under an applied magnetic field of 10 Oe using a superconducting-quantum-interference-device magnetometer (SQUID; Quantum Design: MPMS-XL). The T_c value was defined at the onset temperature of the diamagnetic signal. The superconducting volume fraction was calculated from the field-cooled (FC) magnetization data at 5 K.

Overall oxygen contents of the samples before and after the reductive annealing were determined by the iodometric titration method [36]. Here it is important to bear in mind that iodometric titration (i) is not a phase-specific technique, and moreover, (ii) it actually probes high-valent copper and cerium species rather than oxygen directly. However, once the exact cation composition is known (or assumed) the titration result can be converted into an (overall) oxygen content value in a straightforward manner. On the other hand, in the actual analysis of $(R,\text{Ce})_2\text{CuO}_{4+\delta}$ samples the main source of error/inaccuracy lies in the poor sample solubility in diluted HCl solutions of KI. To ensure the complete dissolution highly concentrated HCl solutions and/or elongated dissolution periods are commonly employed. In both cases the undesirable side reaction is accelerated which occurs between iodide and dissolved oxygen (inevitably present in minute amounts in the solution). Here the advantage of using the EDTA synthesis method became evident: our samples with relatively small grains dissolved much faster than those synthesized through a conventional solid-state synthesis route. Moreover, we carefully searched for the proper experimental conditions for the titration. The

criterion was to find conditions under which a blank titration carried out with the same amount of KI but without the sample material would not produce any iodine (due to the undesirable side reaction). In our titration procedure an accurately weighed sample of ~ 20 mg was dissolved in oxygen-freed (achieved by boiling the solution in N_2 gas flow) relatively diluted (1.0–1.3 M) aqueous HCl solution containing a carefully optimized amount of KI (~ 300 mg). The exact amount of iodine produced through the target reaction between I^- and Ce^{IV} , Cu^{II} , Cu^{III} and O^{-I} species (if present) was then determined using a ~ 0.01 M $Na_2S_2O_3$ solution as the titrant and starch (1 ml; 0.2 m %) as the indicator for the end point. Just before the end point ~ 200 mg KSCN was added to avoid the end-point from being diffuse. Concentration of the $Na_2S_2O_3$ solution was standardized against a standard 1/60 M KIO₃ solution and CuO. Each titration analysis was repeated at least five times with reproducibility better than ± 0.002 for the oxygen content ($4 + \delta$). From the titration result for the (overall) oxygen content, the average valence of Cu was calculated assuming the following valence states for the other elements: Nd^{III} , Ce^{IV} and O^{-II} .

3. Results and discussion

Judging from the XRD patterns (as shown in Fig. 1), the $(Nd_{1-x}Ce_x)_2Cu_{1-y}O_{4+\delta}$ samples as-synthesized in air were of the single $(Nd,Ce)_2CuO_4$ phase with no traces of impurity phases up to $x = 0.10$. Upon increasing the Ce content, both the lattice parameters, a and c , were found to change in a highly linear manner: the a parameter

increases, whereas the c parameter decreases (see the inset of Fig. 1). The decrease in c is straightforwardly explained by the difference in ionic radii of eight-coordinated Nd^{III} (1.109 Å) and Ce^{IV} (0.97 Å) ions [37]. Also agreed is that the increase in a with increasing x is due to the electron-doping effect into the antibonding Cu–O orbital in the CuO_2 plane [23,38].

For each as-air-synthesized sample the post-synthesis reductive annealing was carried out under various partial pressures of oxygen, P_{O_2} . As a final outcome of decreasing the P_{O_2} the $(Nd,Ce)_2CuO_4$ phase was found to decompose into $(Nd,Ce)_2O_3$ and $CuNdO_2$. However, prior to the actual decomposition minute amounts of the $(Nd,Ce)_2O_3$ phase were detected by XRD in all samples. Fig. 2 summarizes the situation in the form of an x -vs.- P_{O_2} phase diagram, where a circle, square, triangle and christcross refer respectively to single-phase $(Nd,Ce)_2CuO_4$, appearance of a minute amount of $(Nd,Ce)_2O_3$, partial decomposition and total decomposition to $(Nd,Ce)_2O_3$ and $CuNdO_2$. From Fig. 2, the stability of the $(Nd,Ce)_2CuO_4$ phase against the decrease in P_{O_2} is enhanced with increasing Ce content. The appearance of minute amounts of $(Nd,Ce)_2O_3$ (found for each sample composition x) before the actual decomposition agrees with the phase-separation scheme suggested in earlier works [13,39–42], i.e. separation of as-synthesized Cu-deficient $(Nd,Ce)_2Cu_{1-y}O_{4+\delta}$ into an essentially cation stoichiometric $(Nd,Ce)_2CuO_{4+\epsilon}$ superconductor and a Cu-free $(Nd,Ce)_2O_3$ minority phase upon the reductive annealing according to Reaction (1). Here we carefully investigated the reversibility of the phase-separation reaction and found

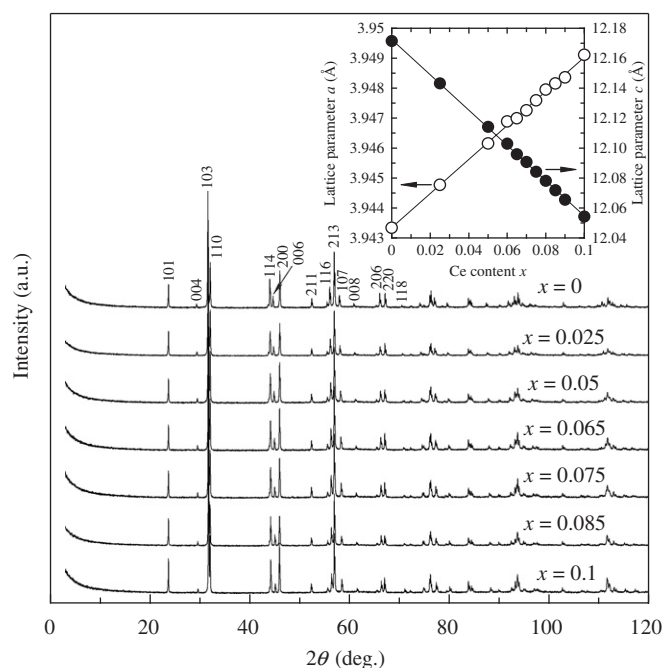


Fig. 1. X-ray diffraction patterns for the as-synthesized samples of $(Nd_{1-x}Ce_x)_2Cu_{1-y}O_{4+\delta}$. Inset shows the variation of lattice parameters, a and c , with the Ce content, x .

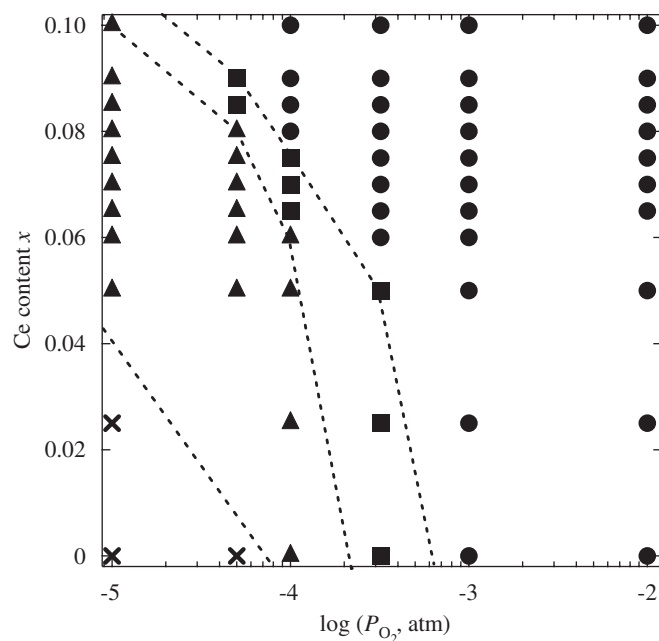


Fig. 2. Phase diagram (Ce content x -vs.- P_{O_2}) for the $(Nd_{1-x}Ce_x)_2Cu_{1-y}O_{4+\delta}$ system. The samples were annealed at 1000 °C for 24 h under the given P_{O_2} (●, stable; ■, phase-separated; ▲, partially-decomposed; ×, decomposed).

that the diffraction peaks due to the $(\text{Nd,Ce})_2\text{O}_3$ phase disappeared (for all the x compositions) when the oxygen-reduced samples were re-oxygenated by annealing in air. The situation is illustrated for $x = 0.075$ in Fig. 3, showing XRD patterns for the same sample powder (i) after the initial synthesis in air, (ii) after the reductive annealing in low-oxygen-pressure atmosphere, and again (iii) after a re-annealing in air. Only in pattern (ii) peaks due to the $(\text{Nd,Ce})_2\text{O}_3$ phase are visible. In order to determine the fraction of the $(\text{Nd,Ce})_2\text{O}_3$ minority phase, the patterns were analyzed through a two-phase Rietveld refinement which revealed the following $(\text{Nd,Ce})_2\text{O}_3$ -phase contents: (i) 0.0 mol%, (ii) 1.6 mol% and (iii) 0.0 mol%.

In Ref. [13], it was convincingly demonstrated that the phase separation reaction is related with the presence of tiny amounts of CuO_2 -plane Cu vacancies in as-air-synthesized samples, see Reaction (1). Apparently the vacancies are due to evaporation of small amounts of copper during the sample synthesis, as no traces of Cu-containing impurity phase(s) were detected in any of our nominally stoichiometric samples. As for the concentration of these vacancies, we may use Reaction (1) to reveal an estimate for the magnitude of y in the as-synthesized $(\text{Nd}_{1-x}\text{Ce}_x)_2\text{Cu}_{1-y}\text{O}_{4+\delta}$ samples (here at ~ 0.016) on the bases of the fraction of the $(\text{Nd,Ce})_2\text{O}_3$ phase in the annealed samples (here 1.6 mol%). Unfortunately, the resolution/sensitivity of the present laboratory — XRD data did not allow us to directly refine the Cu occupancy factors in a reliable manner. Hence, we only refer to the synchrotron X-ray and neutron diffraction study by Kang et al. [13], revealing the magnitude of y at 0.01–0.02 in air-grown $(\text{R,Ce})_2\text{Cu}_{1-y}\text{O}_{4+\delta}$ single crystals.

As for the superconductivity characteristics, it turned out that for each $(\text{Nd}_{1-x}\text{Ce}_x)_2\text{Cu}_{1-y}\text{O}_{4+\delta}$ sample whatever was the value of x , the best superconductivity characteristics (in terms of T_c and volume fraction) were achieved when the sample was annealed in the vicinity of the lowest possible P_{O_2} , i.e. in the region where the first signs of the $(\text{Nd,Ce})_2\text{O}_3$ phase appear in the XRD pattern. Hence, the optimal annealing condition in terms of P_{O_2} differs from sample to sample depending on the Ce content, x . Here the optimal or the lowest possible annealing P_{O_2} at 1000 °C was determined at $\sim 3.2 \times 10^{-4}$ atm for $x \leq 0.06$ and at $\sim 1.0 \times 10^{-4}$ atm for $x \geq 0.065$.

The optimal (= lowest possible) P'_{O_2} s were used to prepare a series of $(\text{Nd}_{1-x}\text{Ce}_x)_2\text{Cu}_{1-y}\text{O}_{4+\delta}$ [or $(1-y)(\text{Nd}_{1-x}\text{Ce}_x)_2\text{CuO}_{4+\varepsilon} + y(\text{Nd}_{1-x}\text{Ce}_x)_2\text{O}_3$] samples with the lowest possible oxygen content for each Ce composition x . It should be emphasized that even though the oxygen-reduced samples include minute amounts of the $(\text{Nd,Ce})_2\text{O}_3$ phase, the overall cation composition is believed to remain constant in Reaction (1) [13]. Hence, the overall sample composition may be expressed by $(\text{Nd}_{1-x}\text{Ce}_x)_2\text{Cu}_{1-y}\text{O}_{4+\delta}$ both before and after the oxygen reduction/phase separation. In Fig. 4, the overall oxygen content values, i.e. $4 + \delta$ in $(\text{Nd}_{1-x}\text{Ce}_x)_2\text{Cu}_{1-y}\text{O}_{4+\delta}$, as calculated from the results of iodometric titration analyses are plotted against x for the maximally reduced samples together with the corresponding as-synthesized samples. Since the exact y value is not known, the result is shown for three different cases assuming $y = 0.00$, 0.01 or 0.02. From Fig. 4, in accordance with the earlier studies on the $(\text{Nd,Ce})_2\text{CuO}_{4+\delta}$ system [29,30], it is found for both the as-synthesized and the maximally-reduced sample series that the overall

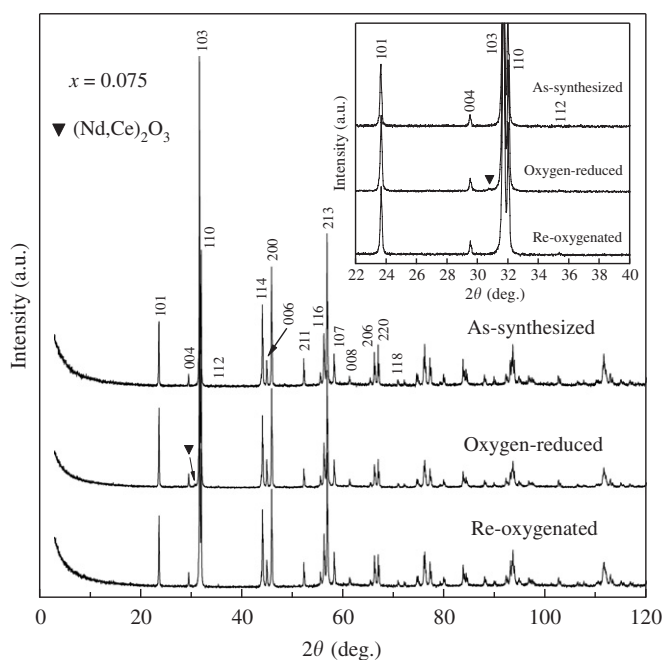


Fig. 3. X-ray diffraction patterns for the $x = 0.075$ sample powder (i) after the initial synthesis in air, (ii) after the reductive annealing in low-oxygen-pressure atmosphere, and again (iii) after a re-annealing in air.

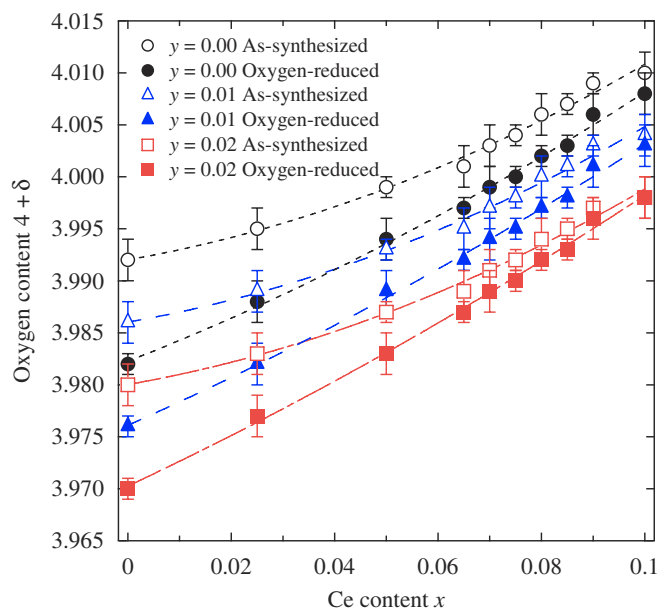


Fig. 4. Oxygen content, $4 + \delta$, plotted against the Ce content x for as-synthesized and oxygen-reduced samples of $(\text{Nd}_{1-x}\text{Ce}_x)_2\text{Cu}_{1-y}\text{O}_{4+\delta}$ assuming $y = 0.00$ (circle), 0.01 (triangle) and 0.02 (square). The samples with $x \leq 0.05$ and $x \geq 0.065$ were annealed at $P_{\text{O}_2} = 3.2 \times 10^{-4}$ and 1.0×10^{-4} atm, respectively.

oxygen content systematically increases with increasing Ce content. Also revealed is that the amount of oxygen lost upon the annealing decreases with increasing x , being ~ 0.01 oxygen atoms *per* formula unit for the non-doped $x=0$ sample and as little as ~ 0.004 for the $x=0.075$ sample. In general, the observed oxygen loss is very tiny, and accordingly the influence of oxygen reduction on the average valence of copper is insignificant (assuming that the valence state of cerium remains constant [43]). For example, a decrease in the oxygen content by 0.004 (as detected for the $x=0.075$ sample upon the reduction annealing) makes the $V(\text{Cu})$ value decrease by 0.008.

From the iodometric titration results (for the overall oxygen content of the sample) meaningful phase-specific oxygen-content values are obtained only for the as-air-synthesized samples that are perfectly single-phasic. In this case too, the precise concentration of Cu vacancies is not known. (Obviously, the larger the y value in reality is, the smaller becomes the oxygen-content value, $4+\delta$, as calculated from the titration data, see Fig. 4). From Fig. 4, it is however clear that the as-air-synthesized $(\text{Nd}_{1-x}\text{Ce}_x)_2\text{Cu}_{1-y}\text{O}_{4+\delta}$ samples are oxygen-deficient, i.e. $4+\delta < 4.00$, at least for $x \leq 0.065$ (i.e. $\delta < 0$ even if $y = 0.00$). On the other hand, if $y = 0.02$, even the $x \geq 0.065$ samples are all oxygen deficient. Needless to say, iodometric titration does not allow us to directly obtain information about the location of the oxygen vacancies. However, a $\delta < 0$ value indicates for sure the presence of oxygen vacancies within either the CuO_2 -plane or the fluorite-structured $(\text{Nd,Ce})\text{-O}_2\text{-(Nd,Ce)}$ block or in both; at the same time, it does not totally rule out the presence of small amounts of defect oxygen atoms at the apical site (which may exist due to a kind of redistribution of some of the oxygen atoms).

In Fig. 5, the lattice parameters, a and c , are plotted against the Ce content for as-synthesized and variously oxygen-reduced samples of $(\text{Nd}_{1-x}\text{Ce}_x)_2\text{Cu}_{1-y}\text{O}_{4+\delta}$. At a fixed Ce content x , the a parameter progressively increases with decreasing P_{O_2} . This trend is particularly evident for the lightly Ce-doped samples: the relative expansion along the a -axis is calculated to be $\sim 0.04\%$ at $x = 0$, while for the heavily Ce-doped samples it is $\sim 0.02\%$. The difference in the magnitude of the a -parameter expansion between the lightly and heavily Ce-doped samples is similar to that of the removal of oxygen (see Fig. 4). The observed lattice expansion along the a -axis upon enhancing the reductive conditions is well explained by the electron-doping effect (though it should be emphasized that the situation is rather complicated since the reduction is apparently accompanied by a simultaneous filling of the Cu vacancies). As for the c -parameter, a systematic contraction is observed for the lightly Ce-doped samples ($\sim 0.05\%$ at $x = 0$), but none for the heavily Ce-doped samples.

Fig. 6 shows the dependence of magnetic susceptibility on temperature for (a) the differently Ce-doped $(\text{Nd}_{1-x}\text{Ce}_x)_2\text{Cu}_{1-y}\text{O}_{4+\delta}$ samples annealed at a constant $P_{\text{O}_2} = 1.0 \times 10^{-4}$ atm, and (b) the $x = 0.075$ samples

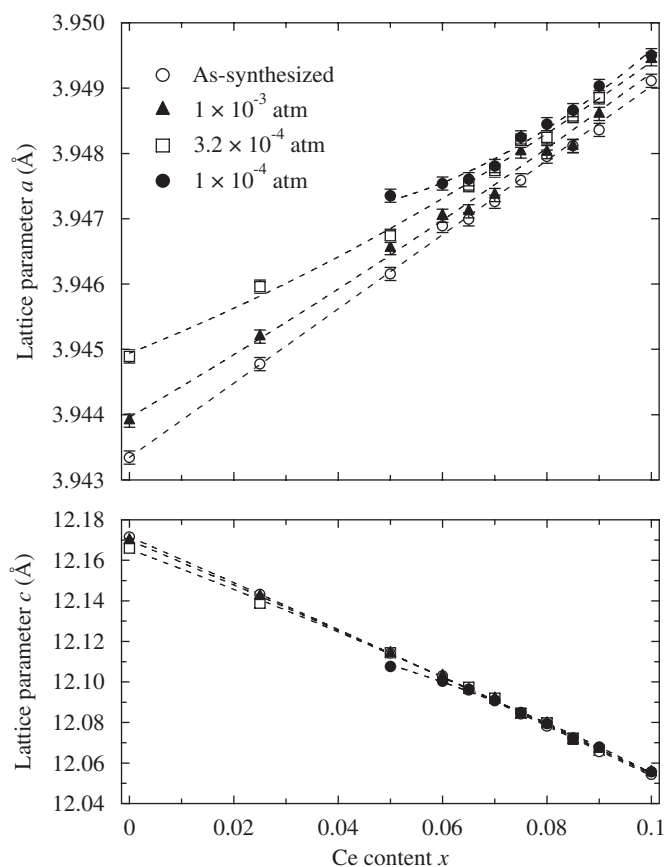


Fig. 5. Lattice parameters, a and c , plotted against the Ce content x for both as-synthesized and oxygen-reduced samples of $(\text{Nd}_{1-x}\text{Ce}_x)_2\text{Cu}_{1-y}\text{O}_{4+\delta}$.

annealed at different P'_{O_2} s. Upon increasing x under the constant- P_{O_2} condition (Fig. 6(a)), the first sign of superconductivity (with a low volume fraction) appears about $x = 0.065$. With further increasing x , superconductivity with the maximum volume fraction shows about $x = 0.075$. With still further increase in x the superconductivity properties gradually get deteriorated. It should be noted that with decreasing x (below $x = 0.075$) the superconducting volume fraction rapidly decreases, while the T_c value remains rather constant. This behavior is consistent with the previous reports for polycrystalline samples [3,26,44], but (particularly for small x values) somewhat contradicting those reported for single crystals [6], probably due to the difference in the reduction processes. On the other hand, when P_{O_2} for the annealing is varied while the Ce content is fixed at $x = 0.075$ (Fig. 6(b)), both the T_c value and the superconducting volume fraction systematically increase with decreasing P_{O_2} down to an optimal value of 1.0×10^{-4} atm and then below this the superconducting volume fraction again starts to decrease due to (partial) phase decomposition.

The T_c value and the superconducting volume fraction for the oxygen-reduced samples are plotted against the Ce content and the annealing P_{O_2} in Figs. 7(a) and (b), respectively. The sample with $x = 0.075$ shows the best

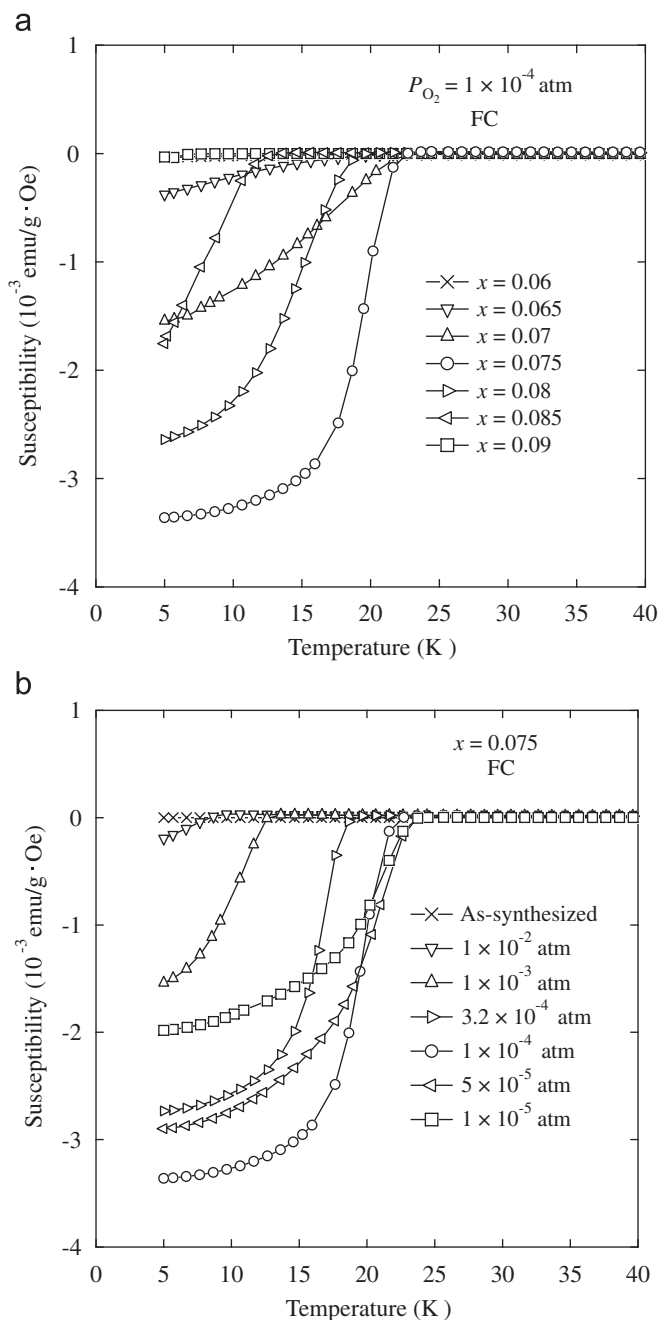


Fig. 6. Temperature dependence of magnetic susceptibility of $(Nd_{1-x}Ce_x)_2Cu_{1-y}O_{4+\delta}$ for (a) samples annealed at a constant $P_{O_2} = 1.0 \times 10^{-4}$ atm and (b) a $x = 0.075$ sample annealed at various P'_{O_2} s.

superconductivity properties for almost all P_{O_2} values (Fig. 7(a)). For the samples with $x \geq 0.075$, the best superconductivity properties are achieved at $P_{O_2} = 1.0 \times 10^{-4}$ atm. On the other hand, samples with $x < 0.075$ show the highest T_c values at $P_{O_2} = 5.0 \times 10^{-5}$ atm, though partial phase decomposition takes place for $P_{O_2} < 5.0 \times 10^{-5}$ atm.

In order to illustrate the importance of oxygen reduction, we plot the T_c values in Fig. 8 against the CuO_2 -plane electron density calculated from the average copper valence value as $n(CuO_2) = 2 - V(Cu)$ for both as-synthesized and

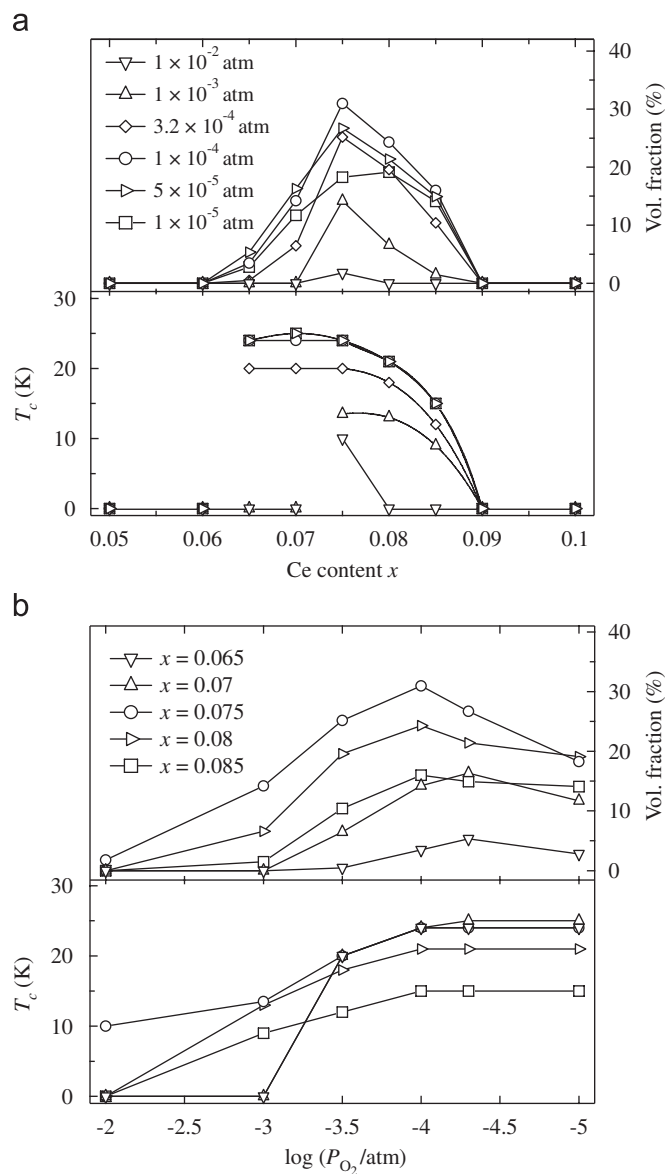


Fig. 7. The T_c value and superconducting volume fraction for oxygen-reduced samples of $(Nd_{1-x}Ce_x)_2Cu_{1-y}O_{4+\delta}$ plotted against (a) Ce content x , and (b) oxygen partial pressure used in the final annealing, P_{O_2} .

oxygen-reduced samples of $(Nd_{1-x}Ce_x)_2Cu_{1-y}O_{4+\delta}$. It is explicitly seen that—in contrast to the p -type high- T_c superconductive copper oxides—the appearance of superconductivity is not determined by the degree of carrier doping only. For instance, the superconductive oxygen-reduced $x = 0.075$ sample has the same $n(CuO_2)$ value as the as-synthesized $x = 0.08$ sample that does not show superconductivity. Hence we conclude that the reduction process should have a significant role other than sufficient electron doping in the course of inducing superconductivity in $(R,Ce)_2Cu_{1-y}O_{4+\delta}$.

4. Conclusion

A large number of high-quality samples (with systematically varied x values) of the electron-doped copper-oxide

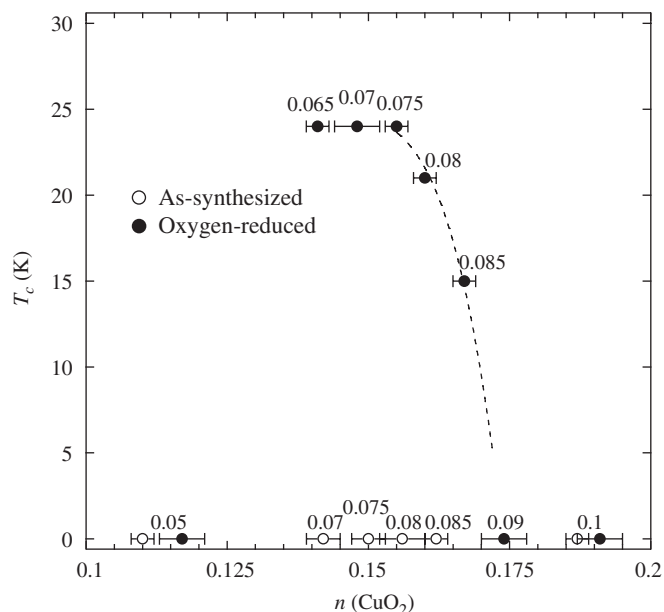


Fig. 8. Relationship between the T_c value and the CuO_2 -plane electron density, $n(\text{CuO}_2) = 2 - V(\text{Cu})$, calculated at $y = 0.00$ for both the as-synthesized and oxygen-reduced samples of $(\text{Nd}_{1-x}\text{Ce}_x)_2\text{Cu}_{1-y}\text{O}_{4+\delta}$. The oxygen-reduction annealing was carried out under $P_{\text{O}_2} = 3.2 \times 10^{-4}$ and 1.0×10^{-4} atm for the samples with $x \leq 0.05$ and $x \geq 0.065$, respectively.

system, $(\text{Nd}_{1-x}\text{Ce}_x)_2\text{Cu}_{1-y}\text{O}_{4+\delta}$, were prepared and characterized for the phase composition, lattice parameters, precise oxygen content and superconductivity characteristics both before and after the low-oxygen-partial-pressure annealing treatments needed to superconductorize the phase. The results obtained are strongly in line with the recently presented phase separation scheme, *i.e.* separation of as-synthesized Cu-deficient $(\text{Nd,Ce})_2\text{Cu}_{1-y}\text{O}_{4+\delta}$ into an essentially cation-stoichiometric superconductor, $(\text{Nd,Ce})_2\text{CuO}_{4+\epsilon}$ and a Cu-free minority phase, $(\text{Nd,Ce})_2\text{O}_3$ upon the reductive annealing treatments [13]. The fraction of the minority phase was estimated at $\sim 1.6\%$ in maximum. Also shown was that the phase separation reaction is reversible, as the diffraction peaks due to the $(\text{Nd,Ce})_2\text{O}_3$ phase disappeared when the oxygen-reduced samples were reoxygenated by annealing in air. Accurate iodometric titrations revealed that the as-air-synthesized (single-phase) samples are oxygen-deficient, *i.e.* $\delta < 0$. Moreover, the amount of oxygen actually removed upon the reductive annealing was found to be extremely small. Accordingly, we may conclude that the impact of the annealing on the valence of copper (and thereby also on the electron doping level) is insignificant. The main outcome of the low-oxygen-partial-pressure annealing seems to be that the copper vacancies present in as-air-synthesized samples are filled, and accordingly minute amounts of Nd and Ce separate as a $(\text{Nd,Ce})_2\text{O}_3$ secondary phase. Note that the fact that successful induction of superconductivity through the low-oxygen-partial-pressure annealing requires very high temperatures ($\sim 1000^\circ\text{C}$) agrees with our conclusion

that the reduction involves diffusion of the (heavier) cations (rather than oxide anions).

Acknowledgments

This work was supported by Academy of Finland (Decision Nos. 110433 and 116254) and also by MSL's International Collaborative Research Project-2007 (Tokyo Tech).

References

- [1] Y. Tokura, H. Takagi, S. Uchida, *Nature* 337 (1989) 345.
- [2] H.k. Müller-Buschbaum, W. Wollschlaeger, *Z. Anorg. Allg. Chem.* 414 (1975) 76.
- [3] H. Takagi, S. Uchida, Y. Tokura, *Phys. Rev. Lett.* 62 (1989) 1197.
- [4] J.M. Longo, P.M. Raccach, *J. Solid State Chem.* 6 (1973) 526.
- [5] K. Hirochi, S. Hayashi, H. Adachi, T. Mitsuyu, T. Hirao, K. Setsune, K. Wasa, *Physica C* 160 (1989) 273.
- [6] T. Uefuji, S. Kuroshima, M. Fujita, K. Yamada, *Physica C* 392 (2003) 189.
- [7] H. Takagi, T. Ido, S. Ishibashi, M. Uota, S. Uchida, Y. Tokura, *Phys. Rev. B* 40 (1989) 2254.
- [8] M. Matsuda, Y. Endoh, K. Yamada, H. Kojima, I. Tanaka, R.J. Birgeneau, M.A. Kastner, G. Shirane, *Phys. Rev. B* 45 (1992) 12548.
- [9] X.Q. Xu, S.N. Mao, W. Jiang, J.L. Peng, R.L. Greene, *Phys. Rev. B* 53 (1996) 871.
- [10] J.S. Higgins, Y. Dagan, M.C. Barr, B.D. Weaver, R.L. Greene, *Phys. Rev. B* 73 (2006) 104510.
- [11] G. Riou, P. Richard, S. Jandl, M. Poirier, P. Fournier, V. Nekvasil, S.N. Barilo, L.A. Kurnevich, *Phys. Rev. B* 69 (2004) 24511.
- [12] P. Richard, G. Riou, I. Hetel, S. Jandl, M. Poirier, P. Fournier, *Phys. Rev. B* 70 (2004) 64513.
- [13] H.J. Kang, P. Dai, B.J. Campbell, P.J. Chupas, S. Rosenkranz, P.L. Lee, Q. Huang, S. Li, S. Komiya, Y. Ando, *Nat. Mater.* 6 (2007) 224; H. Takagi, *Nat. Mater.* 6 (2007) 179.
- [14] P.G. Radaelli, J.D. Jorgensen, A.J. Schultz, J.L. Peng, R.L. Greene, *Phys. Rev. B* 49 (1994) 15322.
- [15] A.J. Schultz, J.D. Jorgensen, J.L. Peng, R.L. Greene, *Phys. Rev. B* 53 (1996) 5157.
- [16] A.N. Petrov, A. Yu. Zuev, T.P. Rodionova, *J. Am. Ceram. Soc.* 82 (1999) 1037.
- [17] F. Izumi, Y. Matsui, H. Takagi, S. Uchida, Y. Tokura, H. Asano, *Physica C* 158 (1989) 433.
- [18] E. Takayama-Muromachi, F. Izumi, Y. Uchida, K. Kato, H. Asano, *Physica C* 159 (1989) 634.
- [19] P. Vigoureux, W. Paulus, M. Barden, A. Cousson, G. Hegger, J.Y. Henry, V. Kvardakov, A. Ivonov, P. Galez, *Physica C* 235 (1994) 1263.
- [20] C. Marin, J.Y. Henry, J.X. Boucherle, *Solid State Commun.* 86 (1993) 425.
- [21] Y. Idemoto, K. Fueki, *Jpn. J. Appl. Phys.* 30 (1991) 2471.
- [22] J.M. Tarascon, E. Wang, L.H. Greene, R. Ramesh, B.G. Bagley, G.W. Hull, P.F. Miceli, Z.Z. Wang, D. Brawner, N.P. Ong, *Physica C* 162 (1989) 285.
- [23] E. Wang, J.-M. Tarascon, L.H. Greene, G.W. Hull, W.R. McKinnon, *Phys. Rev. B* 41 (1990) 6582.
- [24] J.S. Kim, D.R. Gaskell, *Physica C* 209 (1993) 381.
- [25] K. Suzuki, K. Kishio, T. Hasegawa, K. Kitazawa, *Physica C* 166 (1994) 357.
- [26] T. Kawashima, E. Takayama-Muromachi, *Physica C* 219 (1994) 389.
- [27] A. Serquis, F. Prado, A. Caneiro, *Physica C* 313 (1999) 271.
- [28] J.T. Markert, E.A. Early, T. Bjørnholm, S. Ghamaty, B.W. Lee, J.J. Neumeier, R.D. Price, C.L. Seaman, M.B. Maple, *Physica C* 158 (1989) 178.

- [29] E. Moran, A.I. Nazzal, T.C. Huang, J.B. Torrance, *Physica C* 160 (1989) 30.
- [30] T.C. Huang, E. Moran, A.I. Nazzal, J.B. Torrance, P.W. Wang, *Jpn. J. Appl. Phys.* 28 (1989) L1760.
- [31] Y. Idemoto, K. Fueki, T. Shinbo, *Physica C* 166 (1990) 513.
- [32] P.W. Klamut, *J. Alloys Compds.* 194 (1993) L5.
- [33] O.G. Singh, B.D. Padalia, Om. Prakash, K. Suba, A.V. Narlikar, L.C. Gupta, *Physica C* 219 (1994) 156.
- [34] Y.H. Huang, J. Lindén, H. Yamauchi, M. Karppinen, *Chem. Mater.* 16 (2004) 4337.
- [35] V. Petricék, M. Dusek, JANA2000 crystallographic computing system, Inst. Phys. Acad. Sci. Prague Czech Republic (2000).
- [36] M. Karppinen, A. Fukuoka, L. Niinistö, H. Yamauchi, *Supercond. Sci. Technol.* 9 (1996) 121.
- [37] R.D. Shannon, *Acta Crystallogr. A* 32 (1976) 751.
- [38] M.-H. Whangbo, M. Evain, M. Beno, J.M. Williams, *Inorg. Chem.* 26 (1987) 1829.
- [39] F. Prado, J. Briatico, A. Caneiro, M. Tovar, M.T. Causa, *Solid State Commun.* 90 (1994) 695; A. Serquis, F. Prado, A. Caneiro, *Physica C* 313 (1999) 271.
- [40] K. Kurahashi, H. Matsushita, M. Fujita, K. Yamada, *J. Phys. Soc. Jpn.* 71 (2002) 910; H. Kimura, Y. Noda, F. Sato, K. Tsuda, K. Kurahashi, T. Uefuji, M. Fujita, K. Yamada, *J. Phys. Soc. Jpn.* 74 (2005) 2282.
- [41] P.K. Mang, S. Larochelle, A. Mehta, O.P. Vajk, A.S. Erickson, L. Lu, W.J.L. Buyers, A.F. Marshall, K. Prokes, M. Greven, *Phys. Rev. B* 70 (2004) 94507.
- [42] M. Matsuura, P. Dai, H.J. Kang, J.W. Lynn, D.N. Argyriou, K. Prokes, Y. Onose, Y. Tokura, *Phys. Rev. B* 68 (2003) 144503; P. Dai, H.J. Kang, H.A. Mook, M. Matsuura, J.W. Lynn, Y. Kurita, S. Komiya, Y. Ando, *Phys. Rev. B* 71 (2005) R100502.
- [43] Even if we assume that (i) Ce concentration in the (Nd,Ce)₂O₃ minority phase is the same as in the as-synthesized (Nd_{1-x}Ce_x)₂Cu_{1-y}O_{4+δ} sample, and (ii) Ce is trivalent in (Nd,Ce)₂O₃, the corresponding decrease in the average valence of Ce would not significantly affect the value calculated for *V*(Cu) from the iodometrically determined *δ* value.
- [44] P. Lightfoot, D.R. Richards, B. Dabrowski, D.G. Hinks, S. Pei, D.T. Marx, A.W. Mitchell, Y. Zheng, J.D. Jorgensen, *Physica C* 168 (1989) 627.